CHINESE OPTICS LETTERS

Vol. 19, No. 7 | July 2021

High-repetition-rate 1.5 μm passively *Q*-switched Er:Yb:$YAl_3(BO_3)_4$ microchip laser

Songqing Zha (查松青)[1,2], Yujin Chen (陈雨金)[1*], Bingxuan Li (李丙轩)[1,3], Yanfu Lin (林炎富)[1], Wenbin Liao (廖文斌)[1], Yuqi Zou (邹宇琦)[4], Chenghui Huang (黄呈辉)[1], Zhanglang Lin (林长浪)[1], and Ge Zhang (张 戈)[1,3,5**]

[1] Fujian Institute of Research on the Structure of Matter, Chinese Academy of Sciences, Fuzhou 350002, China

[2] Fuzhou University, Fuzhou 350002, China

[3] Fujian Science & Technology Innovation Laboratory for Optoelectronic Information of China, Fuzhou 350108, China

[4] Shanghai Institute of Ceramics, Chinese Academy of Sciences, Shanghai 200050, China

[5] Collaborative Innovation Center for Optoelectronic Semiconductors and Efficient Device, Fuzhou 350108, China

*Corresponding author: cyj@fjirsm.ac.cn

**Corresponding author: zhg@fjirsm.ac.cn

Received October 28, 2020 | Accepted December 21, 2020 | Posted Online March 30, 2021

End-pumped by a 976 nm diode laser, a high-repetition-rate Er : Yb : $YAl_3(BO_3)_4$ microchip laser passively *Q*-switched by a Co^{2+} : $MgAl_2O_4$ crystal is reported. At a quasi-continuous-wave pump power of 20 W, a 1553 nm passively *Q*-switched laser with the repetition rate of 544 kHz, pulse duration of 8.3 ns, and pulse energy of 3.9 μJ was obtained. To the best of our knowledge, the 544 kHz is the highest reported value for the 1.5 μm passively *Q*-switched pulse laser. In the continuous-wave pumping experiment, the maximum repetition rate of 144 kHz with the pulse duration of 8.0 ns and pulse energy of 1.7 μJ was obtained at the incident pump power of 6.3 W.

Keywords: 1.5 μm microchip laser; passive *Q*-switching; Er:Yb:$YAl_3(BO_3)_4$ crystal; high-repetition-rate laser pulse.
DOI: 10.3788/COL202119.071402

1. Introduction

Owing to their great advantages of high sensitivity for Ge, InGaAs, and some novel photodiodes[1–3], as well as excellent transparency in the atmosphere, eye-safe lasers emitting in the 1.5–1.6 μm spectral range have great application prospects in some fields, such as lidar, rangefinder, and three-dimension imaging[4–6]. With rapid development of the unmanned aerial vehicle (UAV) in recent years, vehicular lidars operating at 1.5 μm have attracted wide attention[7–9]. Generally, a vehicular lidar requires excellent laser performances, corresponding to high repetition rate, high pulse energy, and narrow pulse duration. Passive *Q*-switching is a simple and reliable way to achieve a pulse laser with the above properties.

Initial studies on the 1.5 μm laser were mainly based on Er^{3+}/Yb^{3+} co-doped phosphate glasses, which have a lower thermal conductivity of 0.85 $W \cdot m^{-1} \cdot K^{-1}$[10]. The Er:Yb:glass lasers passively *Q*-switched (PQS) by various saturable absorbers (SAs), such as the semiconductor saturable absorption mirror (SESAM)[11,12] and Co^{2+} : $MgAl_2O_4$[13] and Co^{2+} : ZnSe crystals[14], have been reported with repetition rates of 0.5–30 kHz, pulse energies of 1–15 μJ, and pulse durations of 0.8–10 ns. To achieve higher 1.5 μm laser performances, many new Er^{3+}/Yb^{3+} co-doped laser crystals were employed. Among these investigated laser crystals, the Er : Yb : $YAl_3(BO_3)_4$ (Er:Yb:YAB) crystal has been considered as an excellent choice for its high thermal conductivity (7 and 6 $W \cdot m^{-1} \cdot K^{-1}$ along the *a* and *c* axes[10], respectively), high $Yb^{3+} \rightarrow Er^{3+}$ energy transfer efficiency, and weak up-conversion loss[15,16]. The PQS Er:Yb:YAB lasers based on the hemisphere resonator have been reported[17,18], in which the repetition rates were 96 kHz and 105 kHz accompanied by pulse durations of 265 ns and 315 ns, respectively. Then, the microchip laser has been explored to achieve a pulse laser with shorter duration. The PQS Er:Yb:YAB microchip laser with the pulse duration of 5 ns, repetition rate of 60 kHz, and energy of 5.25 μJ has been firstly reported[19]. Some investigations have shown that the Er:Yb:YAB laser performances were restricted by the strong heat loading originating from the large quantum defect and low fluorescence quantum efficiency of the $^4I_{13/2}$ upper laser level[16,20]. To reduce the heat loading, a sapphire crystal with a thermal conductivity of ~40 $W \cdot m^{-1} \cdot K^{-1}$[21] has been used[22], and then a 1.5 μm microchip laser with the energy of 10 μJ, repetition rate of 77 kHz, and pulse duration of 7 ns has been obtained. A Co^{2+} : $MgAl_2O_4$ crystal was used as the SA in the

above-mentioned PQS Er:Yb:YAB lasers, and the realized repetition rates were all lower than 200 kHz.

In addition to Er:Yb:YAB lasers, $Er:Yb:GdAl_3(BO_3)_4$ (Er:Yb:GdAB) crystals were also employed in the 1.5 μm PQS lasers. The PQS Er:Yb:GdAB lasers based on the $Co^{2+}:MgAl_2O_4$ crystal have been reported[23,24], corresponding to the repetition rates of 1–40 kHz, pulse energies of 5–30 μJ, and pulse durations of 1–6 ns. Recently, some two-dimensional nanomaterials, such as the single-walled carbon nanotube (SWCNT)[25] and single-layer graphene[26], have also been used as SAs in the PQS Er:Yb:GdAB laser. The maximum repetition rates of 400–500 kHz were obtained, however, accompanied with pulse durations larger than 100 ns and energies lower than 1 μJ.

Therefore, it is still a challenge to obtain a high-repetition-rate 1.5 μm pulse laser with narrow duration and high energy. In this paper, a 1553 nm Er:Yb:YAB microchip laser with a repetition rate of 544 kHz, pulse duration of 8.3 ns, and energy of 3.9 μJ was reported. To the best of our knowledge, the 544 kHz is the highest reported value for the 1.5 μm PQS pulse laser. The vehicular lidar with high repetition rate contributes to achieving high speed of scanning. Considering its cheap and compact characteristics, the reported 1553 nm microchip laser has a promising application in the lidar used in UAVs.

2. Materials and Methods

2.1. Laser crystal and saturable absorber

An Er(atomic fraction of 1.5%):Yb(atomic fraction of 12%):YAB crystal was employed as the laser gain medium in this experiment, and the detailed crystal growth procedure has been reported[27]. The Er:Yb:YAB crystal is an optically uniaxial crystal, which is characterized for two principal light polarizations, $E \| c(\pi)$ and $E \perp c(\sigma)$ (the optical axis is parallel to the c axis). The polarized absorption spectra in the 700–1700 nm range are shown in Fig. 1(a), which were recorded by a UV-visible (VIS)-near-IR (NIR) spectrophotometer (Lambda-950, PerkinElmer). The absorption coefficient due to σ polarization is much larger than that of π polarization, and a c-cut Er:Yb:YAB crystal with dimensions of 3 mm × 3 mm × 1.5 mm was used in this experiment.

A $Co^{2+}:MgAl_2O_4$ crystal with dimensions of 3 mm × 3 mm × 1.3 mm was used as the SA in this experiment. Its transmission spectrum is shown Fig. 1(b), and the initial transmission T_{SA} at 1.5 μm was about 95.8%.

2.2. Microchip laser setup

The microchip laser setup is shown in Fig. 2. The input mirror (IM) and the output coupler (OC) were coated on the surfaces of two sapphire crystals, which acted as the heat sinks in the microchip laser. These sapphire crystals with a cross section of 3 mm × 3 mm were polished to achieve a high surface quality with the parallelism better than 20 arcsec. The IM was antireflection-coated at 800–1000 nm with a high reflectivity of 99.8% at 1500–1600 nm. The OC had a transmission of 6% at

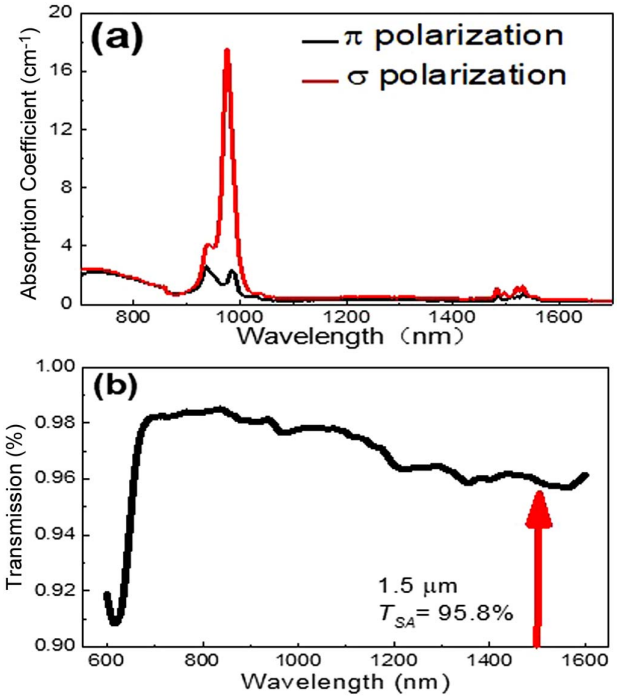

Fig. 1. Material properties of the laser crystal and SA. (a) Polarized absorption spectra of the Er:Yb:YAB crystal and (b) transmission spectrum T_{SA} of the employed Co^{2+}: $MgAl_2O_4$ crystal.

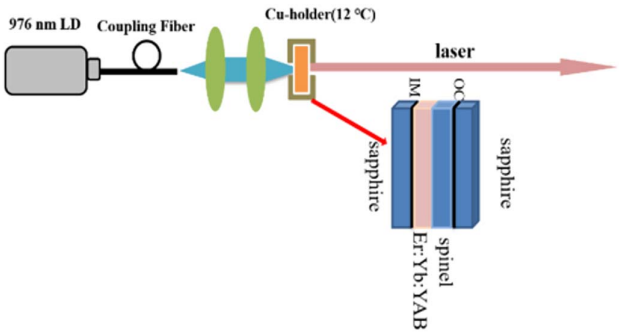

Fig. 2. Experimental setup for the PQS Er:Yb:YAB microchip laser.

1500–1600 nm. The IM and the OC were tightly attached to the surfaces of the Er:Yb:YAB and $Co^{2+}:MgAl_2O_4$ crystals, respectively. Therefore, the resonator length was 2.8 mm. The resonator was mounted inside a copper holder cooled at 12°C and tightly pressed by screws. There was a hole with a radius of about 0.75 mm in the center of the holder to permit the passing of pumping laser beams.

In our previous experiment, the 77 kHz microchip laser[22] was generated under a fiber-coupled laser diode (LD) with a maximum output power of 8 W (central wavelength: 975.4 nm, core diameter: 100 μm, and numerical aperture: 0.15). In this work, the performances of the microchip laser were explored under a new LD with a maximum output power of 20 W (central wavelength: 975.5 nm, core diameter: 105 μm,

and numerical aperture: 0.22). After passing a lens assembly, the pump beam was focused into the laser crystal with a radius of about 60 μm. Caused by the thermal expansion of the laser crystal, the IM, which was coated on the laser crystal in a previous laser configuration, was easily damaged under high incident pump power. Therefore, the IM was coated on the sapphire crystal in our new microchip laser configuration. Firstly, the microchip laser was pumped by the continuous-wave (CW) LD, and the thermal damage of the laser crystal appeared under high incident power. The performances of the microchip laser were limited by the strong heat loading. In order to reduce the heat loading, the microchip laser was pumped by the quasi-CW (QCW) LD, and a 544 kHz pulse laser was obtained.

3. Results and Discussion

3.1. CW pumping experiment

The new microchip laser performances were firstly investigated under CW pumping. The dependence of the laser characteristics on the incident pump power is shown in Fig. 3. The laser threshold was 2.2 W. The average output power and repetition rate of the microchip laser were increased with the increment of the incident pump power from 2.2 W to 4.5 W. When the incident pump power was further increased from 4.5 W, the average output power and repetition rate of the microchip laser could not be obviously increased, and the bending of output characteristics was observed. In order to avoid the thermal damage of the laser crystal, the microchip laser operated under incident pump power lower than 6.8 W. For all incident pump power, the pulse energy was kept at 1–4 μJ, and the pulse duration was kept at 7–9 ns. In the CW pumping experiment, the microchip laser with the maximum repetition rate of 144 kHz, pulse duration of 8.0 ns, and pulse energy of 1.7 μJ was obtained at the incident pump power of 6.3 W. The pulse train is shown in the Fig. 4(a). The pulse operation was stable, and the amplitude variations between various pulses and interpulse time jittering were kept within 5%. The single-pulse profile is shown in Fig. 4(b), and the full width at half-maximum (FWHM) of the laser pulse is 8.0 ns. The oscillating wavelength of the pulse laser was centered at about 1548 nm, which is shown in the inset of Fig. 4(b).

Pumped by the CW LD, a microchip laser with the maximum repetition rate of 144 kHz, duration of 8.0 ns, and energy of 1.7 μJ was obtained, and the repetition rate of the microchip laser could not be further increased. Compared with the previous reports about 1.5 μm pulse lasers based on a hemisphere resonator[17,18] or using two-dimensional nanomaterials as

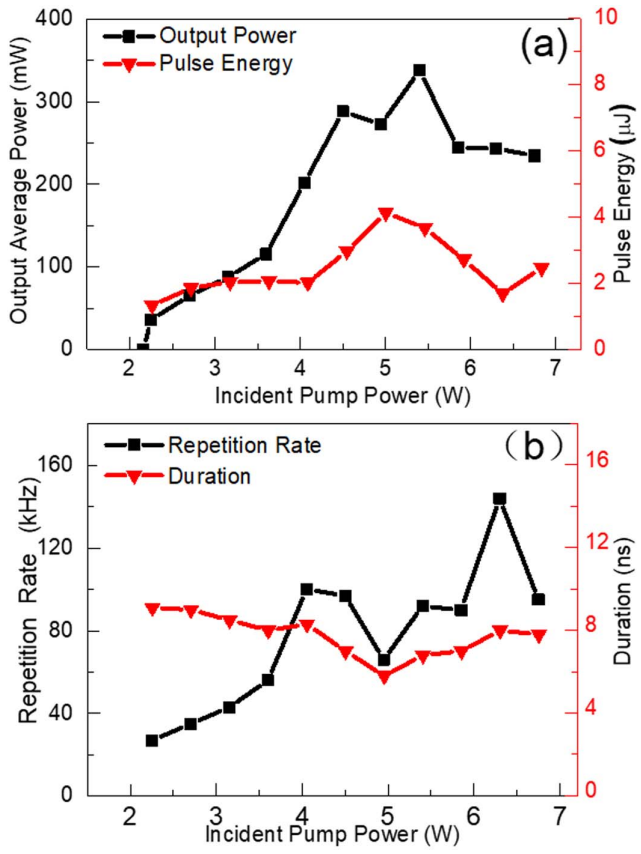

Fig. 3. Microchip laser pumped by a CW LD. (a) Average output power and pulse energy and (b) pulse repetition rate and pulse duration versus incident pump power.

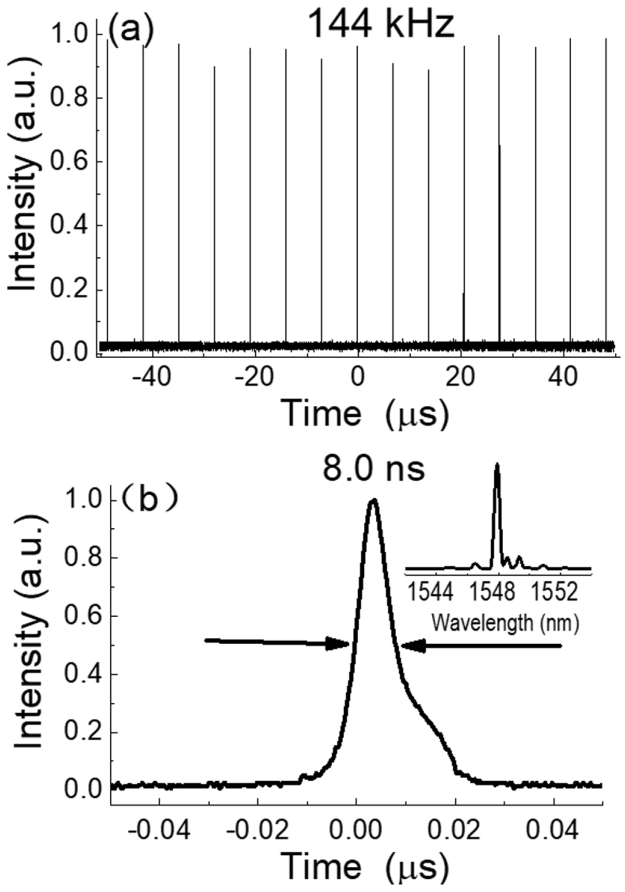

Fig. 4. Microchip laser operated at the incident power of 6.3 W. (a) Pulse train profile and the pulse repetition rate. (b) Single-pulse profile and pulse duration; the inset shows the laser spectrum.

SAs[25,26], the microchip laser with the $Co^{2+}:MgAl_2O_4$ crystal as the SA showed a strong advantage for achieving a narrower pulse duration. The pulse duration in this experiment (about 8 ns) was one order of magnitude lower than those of these above-mentioned reports (more than 100 ns). In addition, this experiment showed the bending of the output characteristics in 1.5 μm microchip laser operation. Because of the insufficient incident power, the bending of the output characteristics was not observed in the previous microchip laser experiments[19,22].

Owing to the large quantum defect and low fluorescence quantum efficiency of the $^4I_{13/2}$ upper laser level, the generated heat loading was considered as a crucial reason for the bending of the output characteristics. The influences of the heat loading were mainly from two aspects. (1) The stabilization of the microchip laser was typically ensured by a positive thermal lens of the gain material. With the increment of the incident pump power, the strong heat loading increased the thermal lens effect and shortened the thermal focal length. This change induced the mode matching in the microchip laser to become worse. (2) The energy level structure and main transitions in the Er:YB:YAB crystal are shown in the Fig. 5. The heat loading in the microchip laser supplied energy for Er^{3+} in the ground state and forced it to transit to the $^4I_{15/2}$ lower laser level. This process decreased the ratio of Er^{3+} population in the $^4I_{13/2}$ upper and $^4I_{15/2}$ lower laser levels and weakened the laser operation.

Due to the above reasons, the gain of the laser crystal could not be obviously increased when the incident pump power was further increased from 4.5 W. Therefore, the average output power and repetition rate could not be obviously increased, and the bending of the output characteristics would be observed. As for the fluctuation of the output characteristics, it was mainly caused by the generation of the laser with the high-order transverse mode in the laser operation. The generation of the laser with the high-order transverse mode affects the mode matching in the microchip laser and leads to the gain of the laser crystal appearing with slight fluctuations. Therefore, the average output power and repetition rate would appear as fluctuating.

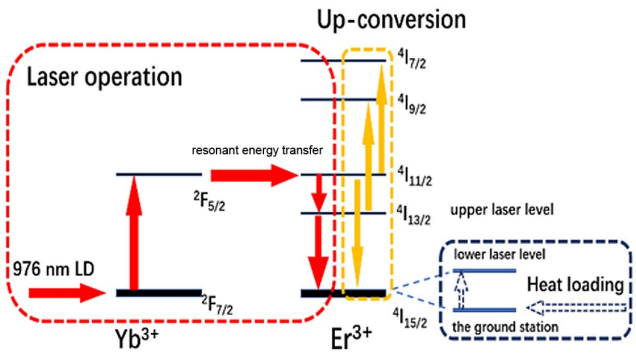

Fig. 5. Energy level structure and main transitions in the Er:Yb:YAB laser.

3.2. QCW pumping experiment

In order to reduce the heat loading, the microchip laser was pumped by a QCW LD. In this case, the thermal damage of the Er:Yb:YAB crystal could be effectively avoided and a higher-peak-power LD could be employed in the microchip laser. When the Er:Yb:YAB laser crystal was pumped by a higher-peak-power LD, the pumping rate of the Er^{3+} ions that transited from the ground state to the $^4I_{13/2}$ upper laser level would be increased, and then the energy storage time of the $^4I_{13/2}$ upper laser level would be reduced. Therefore, an LD with higher peak power could reduce the interpulse time and increase the repetition rate of the output pulse. The results of the QCW pumping experiment are shown in Figs. 6 and 7.

In the QCW pumping experiment, the microchip laser was pumped by a QCW LD with the pulse period of 2 ms and a duty-cycle of 20%. It can be seen from Fig. 6(a) that the laser threshold was at a peak power of 2 W. The average output power was linearly increased with the increment of the pump peak power, and the pulse energy was always kept at 3–6 μJ. Figure 6(b) showed that the pulse repetition rate was increased with the increment of the pump peak power from 2 W to 20 W. The pulse duration was decreased from 34 ns to 9.8 ns with the increment of the pump peak power from 2 W to 10 W. In our opinion, the weaker thermal lens effect would lead the microchip laser to be operated with a larger laser mode area and a lower power density, so the SA was not fully bleached at the threshold

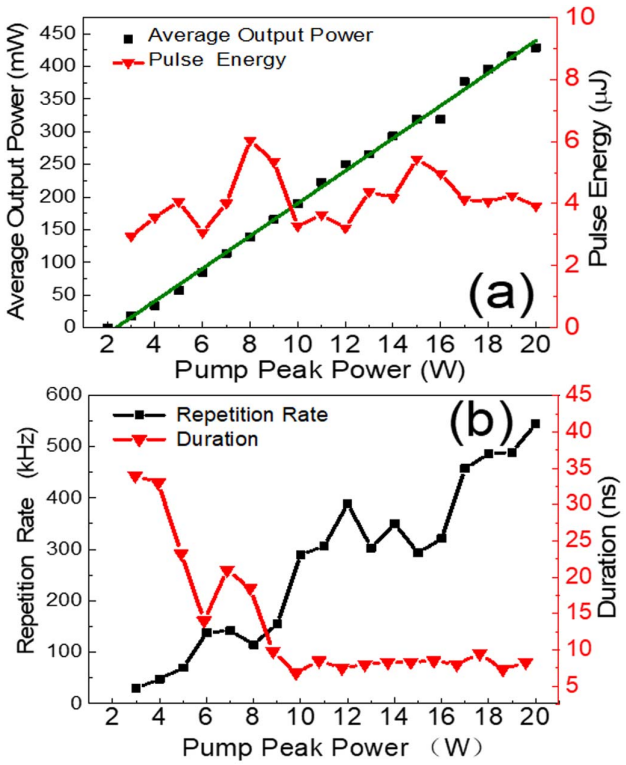

Fig. 6. Microchip laser pumped by a QCW LD. (a) Average output power and pulse energy and (b) pulse repetition rate and pulse duration versus pump peak power.

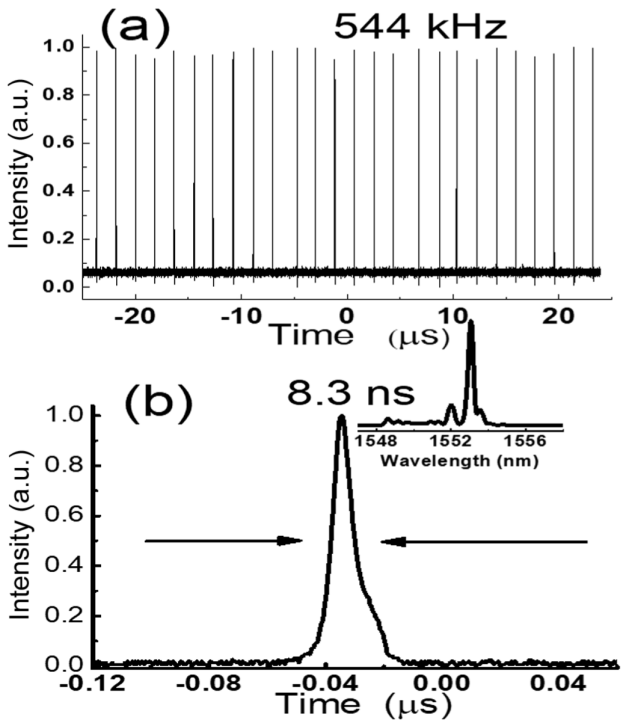

Fig. 7. Microchip laser operated at the QCW pump power of 20 W. (a) Pulse train profile and the pulse repetition rate. (b) Single-pulse profile and pulse duration; the inset shows the laser spectrum.

under QCW pumping mode. The pulse duration could be written as

$$\tau_P = \frac{7nL}{c\Delta R}.$$

Then, the thermal lens effect and ΔR (the modulation depth of the SA) would be increased when the QCW pump power increased from 2 W to 10 W. Therefore, a huge fluctuation of the pulse duration appeared. When the pump peak power was further increased from 10 W to 20 W, the SA was fully bleached, and the pulse duration was kept at 8–9 ns. No bending of the output characteristics of the average output power and repetition rate was observed. By comparing Figs. 3 and 6, it can be found that the repetition rate of the CW pumping microchip laser was seriously limited by the heat loading of the laser crystal. When the heat loading was greatly reduced, the higher-peak-power pump would induce a higher-repetition-rate laser operation. These experimental results were in agreement with the previous analysis.

At the pump peak power of 20 W, a microchip pulse laser with the repetition rate of 544 kHz, duration of 8.3 ns, and energy of 3.9 μJ was successfully obtained. The pulse train is shown in Fig. 7(a), where the amplitude variations between various pulses and interpulse time jittering were about 10%. The pulse profile is shown in Fig. 7(b), and the FWHM of the laser pulse was 8.3 ns. The laser spectrum is shown in the inset of the Fig. 7(b), and the oscillating wavelength of the pulse laser was centered at about 1553 nm. To the best of our knowledge, the 544 kHz is the highest reported value for the 1.5 μm PQS pulse laser. The maximum peak power of 20 W in the experiment was limited by the available pump source in our laboratory. According to the trend of the repetition rate shown in Fig. 6(b), it could be expected that a 1.5 μm pulse laser with a repetition rate more than 544 kHz would be obtained when the microchip laser was pumped by a QCW LD with a higher peak power.

4. Conclusion

A 1.5 μm PQS laser with the repetition rate of 544 kHz, pulse duration of 8.3 ns, and pulse energy of 3.9 μJ was obtained, and the great potential of the Er:Yb:YAB microchip laser to achieve a higher-repetition-rate 1.5 μm pulse laser was displayed in the QCW pumping experiment. However, the maximum repetition rate of the microchip laser in the CW pumping experiment was only 144 kHz, which was restricted by the heat loading. Our experiment promoted the study and development of the high-repetition-rate 1.5 μm pulse laser. The lidar with high repetition rate contributes to achieving a high speed of scanning. Considering its cheap and compact characteristics, the reported 1553 nm microchip laser has a promising application in the lidar used in UAVs.

Acknowledgement

This work was supported by the National Natural Science Foundation of China (Nos. 61875199 and 61975208), Strategic Priority Research Program of the Chinese Academy of Sciences (No. XDB20000000), and Science and Technology Service Network Initiative of the Chinese Academy of Sciences (No. KFJ-STS-QYZX-069).

References

1. D. Wu, J. W. Guo, J. Du, C. X. Xia, L. H. Zeng, Y. Z. Tian, Z. F. Shi, Y. T. Tian, X. J. Li, Y. H. Tsang, and J. S. Jie, "Highly polarization-sensitive, broadband, self-powered photodetector based on graphene/$PdSe_2$/germanium heterojunction," ACS Nano **13**, 9907 (2019).
2. L. H. Zeng, S. H. Lin, Z. H. Lou, H. Y. Yuan, H. Long, Y. Y. Li, W. Lu, S. P. Lau, D. Wu, and Y. H. Tsang, "Ultrafast and sensitive photodetector based on a $PtSe_2$/silicon nanowire array heterojunction with a multiband spectral response from 200 to 1550 nm," NPG Asia Mater. **10**, 352 (2018).
3. L. H. Zeng, D. Wu, S. H. Lin, C. Xie, H. Y. Yuan, W. Lu, S. P. Lau, Y. Chai, L. B. Luo, Z. J. Li, and Y. H. Tsang, "Controlled synthesis of 2D palladium diselenide for sensitive photodetector applications," Adv. Funct. Mater. **29**, 1806878 (2019).
4. M. J. Myers, J. D. Myers, J. T. Sarracino, C. R. Hardy, B. P. Guo, S. M. Christian, J. A. Myers, F. Roth, and A. G. Myers, "LIBS system with compact fiber spectrometer, head mounted spectra display and hand held eye-safe erbium glass laser gun," Proc. SPIE **7578**, 75782G (2010).
5. G. Karlsson, F. Laurell, J. Tellefsen, B. Denker, B. Galagan, V. Osiko, and S. Sverchkov, "Development and characterization of Yb-Er laser glass for high average power laser diode pumping," Appl. Phys. B **75**, 41 (2002).
6. P. Laporta, S. Taccheo, S. Longhi, O. Svelto, and C. Svelto, "Erbium-ytterbium microlasers: optical properties and lasing characteristics," Opt. Mater. **11**, 269 (1999).

7. Q. He, F. Wang, Z. Lin, C. Shao, M. Wang, S. Wang, C. Yu, and L. Hu, "Temperature dependence of spectral and laser properties of Er^{3+}/Al^{3+} co-doped aluminosilicate fiber," Chin. Opt. Lett. **17**, 101401 (2019).
8. H. Liu, Y. Yu, D. Sun, H. Liu, Y. Wang, H. Zheng, D. Li, and G. Jin, "1514 nm eye-safe passively Q switched self-optical parametric oscillator based on Nd^{3+} doped MgO:PPLN," Chin. Opt. Lett. **17**, 111404 (2019).
9. M. Liu, Y. Ouyang, H. Hou, W. Liu, and Z. Wei, "*Q*-switched fiber laser operating at 1.5 μm based on WTe_2," Chin. Opt. Lett. **17**, 020006 (2019).
10. N. A. Tolstik, G. Huber, V. V. Maltsev, N. I. Leonyuk, and N. V. Kuleshov, "Excited state absorption, energy levels, and thermal conductivity of Er^{3+}: YAB," Appl. Phys. B **92**, 567 (2008).
11. R. Fluck, R. Haring, R. Paschotta, E. Gini, H. Melchior, and U. Keller, "Eyesafe pulsed microchip laser using semiconductor saturable absorber mirrors," Appl. Phys. Lett. **72**, 3273 (1998).
12. R. Haring, R. Paschotta, R. Fluck, E. Gini, H. Melchior, and U. Keller, "Passively *Q*-switched microchip laser at 1.5 μm," J. Opt. Soc. Am. B **18**, 1805 (2001).
13. G. Karlsson, V. Pasiskevicius, F. Laurell, J. A. Tellefsen, B. Denker, B. I. Galagan, V. V. Osiko, and S. Sverchkov, "Diode-pumped Er-Yb: glass laser passively Q switched by use of Co^{2+}: $MgAl_2O_4$ as a saturable absorber," Appl. Opt. **39**, 6188 (2000).
14. V. E. Kisel, V. G. Shcherbitsky, N. V. Kuleshov, V. I. Konstantinov, V. I. Levchenko, E. Sorokin, and I. Sorokina, "Spectral kinetic properties and lasing characteristics of diode-pumped Cr^{2+}:ZnSe single crystals," Opt. Spectrosc. **99**, 663 (2005).
15. N. A. Tolstik, V. E. Kisel, N. V. Kuleshov, V. V. Maltsev, and N. I. Leonyuk, "Er,Yb:$YAl_3(BO_3)_4$ efficient 1.5 μm laser crystal," Appl. Phys. B **97**, 357 (2009).
16. N. A. Tolstik, S. V. Kurilchik, V. E. Kisel, N. V. Kuleshov, V. V. Maltsev, O. V. Pilipenko, E. V. Koporulina, and N. I. Leonyuk, "Efficient 1 W continuous-wave diode-pumped Er,Yb:$YAl_3(BO_3)_4$ laser," Opt. Lett. **32**, 3233 (2007).
17. Y. J. Chen, Y. F. Lin, Y. Q. Zou, J. H. Huang, X. H. Gong, Z. D. Luo, and Y. D. Huang, "Diode-Pumped 1.5–1.6 μm laser operation in Er^{3+} doped $YAl_3(BO_3)_4$ microchip," Opt. Express **22**, 13969 (2014).
18. Y. J. Chen, Y. F. Lin, J. H. Huang, X. H. Gong, Z. D. Luo, and Y. D. Huang, "Efficient continuous-wave and passively *Q*-switched pulse laser operations in a diffusion-bonded sapphire/Er:Yb:$YAl_3(BO_3)_4$/sapphire composite crystal around 1.55 μm," Opt. Express **26**, 419 (2018).
19. V. E. Kisel, K. N. Gorbachenya, A. S. Yasukevich, A. M. Ivashko, N. V. Kuleshov, V. V. Maltsev, and N. I. Leonyuk, "Passively *Q*-switched microchip Er,Yb:$YAl_3(BO_3)_4$ diode-pumped laser," Opt. Lett. **37**, 2745 (2012).
20. Y. J. Chen, Y. F. Lin, J. H. Huang, X. H. Gong, Z. D. Luo, and Y. D. Huang, "Enhanced performances of diode-pumped sapphire/Er^{3+}:Yb^{3+}:$LuAl_3(BO_3)_4$/sapphire micro-laser at 1.5–1.6 μm," Opt. Express **23**, 12401 (2015).
21. C. Rothhardt, J. Rothhardt, A. Klenke, T. Peschel, R. Eberhardt, J. Limpert, and A. Tunnermann, "BBO-sapphire sandwich structure for frequency conversion of high power lasers," Opt. Mater. Express **4**, 1092 (2014).
22. Y. Chen, Y. Lin, Z. Yang, J. Huang, X. Gong, Z. Luo, and Y. Huang, "Eye-safe 1.55 μm Er:Yb:$YAl_3(BO_3)_4$ microchip laser," OSA Continuum. **2**, 142 (2019).
23. K. N. Gorbachenya, V. E. Kisel, A. S. Yasukevich, V. V. Maltsev, N. I. Leonyuk, and N. V. Kuleshov, "Highly efficient continuous-wave diode-pumped Er,Yb:$GdAl_3(BO_3)_4$ laser," Opt. Lett. **38**, 2446 (2013).
24. D. D. Mitina, V. V. Maltsev, N. I. Leonyuk, K. N. Gorbachenya, R. V. Deineka, V. E. Kisel, A. S. Yasukevich, and N. V. Kuleshov, "Growth and characterization of $RMgB_5O_{10}$ (R = Y, La, Gd) crystals," Inorg. Mater. **56**, 211 (2020).
25. K. N. Gorbachenya, V. E. Kisel, A. S. Yasukevich, M. B. Prudnikova, V. V. Maltsev, N. I. Leonyuk, S. Y. Choi, F. Rotermund, and N. V. Kuleshov, "Passively *Q*-switched Er,Yb:$GdAl_3(BO_3)_4$ laser with single-walled carbon nanotube based saturable absorber," Laser Phys. Lett. **14**, 035802 (2017).
26. K. Gorbachenya, V. Kisel, A. Yasukevich, P. Loiko, X. Mateos, V. Maltsev, N. Leonyuk, M. Aguilo, F. Diaz, U. Griebner, V. Petrov, and N. Kuleshov, "Graphene *Q*-switched Er,Yb:Gd $Al_3(BO_3)_4$ laser at 1550 nm," Appl. Opt. **56**, 4745 (2017).
27. W. X. You, Y. F. Lin, Y. J. Chen, Z. D. Luo, and Y. D. Huang, "Growth and spectroscopic properties of Er^{3+} single doped and Er^{3+}-Yb^{3+} co-doped $YAl_3(BO_3)_4$ crystals," J. Crystal Growth **270**, 481 (2004).